

Type IV Secretion System Core Component VirB8 from *Brucella* Binds to the Globular Domain of VirB5 and to a Periplasmic Domain of VirB6

Ana Maria Villamil Giraldo,[†] Durga Sivanesan,[†] Anna Carle,[‡] Athanasios Paschos,[§] Mark A. Smith,[†] Maria Plesa,^{||} James Coulton,^{||} and Christian Baron^{*,†}

[†]Department of Biochemistry, Université de Montréal, C.P. 6128, Succ. Centre-ville, Montréal, QC H3C 3J7, Canada

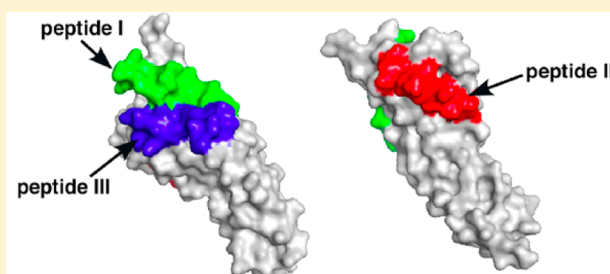
[‡]Department Biologie I, Bereich Mikrobiologie, Ludwig-Maximilians-Universität, Maria-Ward-Strasse 1a, D-80638 Munich, Germany

[§]Department of Biology, McMaster University, 1280 Main Street West, Hamilton, ON L8S 4K1, Canada

^{||}Department of Microbiology and Immunology, McGill University, 3775 University Street, Montréal, QC H3A 2B4, Canada

S Supporting Information

ABSTRACT: Type IV secretion systems are macromolecular assemblies in the cell envelopes of bacteria that function in macromolecular translocation. Structural biology approaches have provided insights into the interaction of core complex components, but information about proteins that undergo transient interactions with membrane components has not been forthcoming. We have pursued an unbiased approach using peptide arrays and phage display to identify interaction partners and interaction domains of type IV secretion system assembly factor VirB8. These approaches identified the globular domain from the VirB5 protein to interact with VirB8. This interaction was confirmed in cross-linking, pull-down, and fluorescence resonance energy transfer (FRET)-based interaction assays. In addition, using phage display analysis, we identified different regions of VirB6 as potential interaction partners of VirB8. Using a FRET-based interaction assay, we provide the first direct experimental evidence of the interaction of a VirB6 periplasmic domain with VirB8. These results will allow us to conduct directed structural biological work and structure–function analyses aimed at defining the molecular details and biological significance of these interactions with VirB8 in the future.



Protein–protein interactions between subunits of complex translocation machineries such as secretion systems play key roles in providing complex assembly, stability, and function. On the basis of their protein composition and mechanism, bacterial secretion systems are grouped into seven categories, and many systems contribute to bacterial virulence and survival within the host organism. We here present the results of an unbiased search for interaction partners of the VirB8 protein from the type IV secretion system (T4SS) from the human and animal pathogen *Brucella*. Many Gram-negative pathogens possess T4SSs that are required for virulence, e.g., *Agrobacterium tumefaciens*, *Bartonella* species, *Bordetella pertussis*, *Brucella* species, *Helicobacter pylori*, and *Legionella pneumophila*.^{1–3} T4SSs traverse the inner and outer membrane and translocate proteins or DNA–protein complexes from Gram-negative bacteria. The best characterized T4SS model is from the plant pathogen *A. tumefaciens*, but the work reported here was conducted with *Brucella* VirB proteins as they are more suited for purification and in vitro biochemical studies.^{4,5} *Brucella* requires its T4SS for infection (survival and replication) of mammalian cells.⁶ Similarly, T4SSs are required for the transfer of antibiotic resistance gene-carrying plasmids between bacteria.

T4SSs consist of three groups of proteins: ATPases, core components, and surface-exposed components. The ATPases (VirB4, VirB11, and VirD4) are localized mainly in the cytoplasm, but they traverse the membrane and energize the translocation machinery.^{7–9} The core components (VirB6–VirB10) bridge the inner and outer membrane and are linked to the surface-exposed pilus components (VirB2 and VirB5).^{4,10–16} Structural biological approaches [X-ray crystallography and nuclear magnetic resonance (NMR) spectroscopy] have revealed the structures of domains or full-length individual T4SS components (VirB5, VirB8–VirB11, and VirD4^{17–22}), and recent cryo-EM and X-ray crystallography work has revealed the structure of the T4SS core complex comprised of VirB7, VirB9, and VirB10.^{23,24} The core complex forms a conduit for the translocation of substrates across the cell envelope, and an energy-dependent change in the conformation of VirB10 is believed to accompany this process.⁷

VirB8 is not part of the core complex but is essential for T4SS assembly in vivo. VirB8 interacts with many different

Received: March 1, 2012

Revised: April 17, 2012

Published: April 19, 2012

VirB proteins (VirB1, VirB4, VirB5, and VirB9–VirB11) and is believed to function as an assembly factor for the secretion system.^{4,5,25–28} VirB8 and VirB10 are bitopic inner membrane proteins with short 32–43-amino acid N-termini, one transmembrane helix, and 177- and 339-amino acid periplasmic regions, respectively. They were shown to form homo- and heterodimers and also interact with the VirB9 protein, which led to the proposal of a sequence of interactions that contribute to T4SS assembly.²⁹ VirB6 is the most hydrophobic T4SS component; it stabilizes VirB5 and VirB3, is believed to contain at least four transmembrane helices, and was proposed to be the channel for secretion system function.^{16,30–32} However, so far, there is no direct evidence of this notion, but VirB6 and VirB8 were shown to act at a common step of DNA substrate translocation from *Agrobacterium*.³³ VirB5-like proteins are minor components of T4SS-determined surface structures such as the *Agrobacterium* T-pilus and were previously shown to interact with VirB8.^{4,13,14,34}

VirB8 is an inner membrane protein, and considering that the final localization of VirB5 is on the cell surface, it likely engages in a transient interaction leading to T-pilus assembly. Structures of VirB5 and VirB8 homologues are available,^{17,18,35} but considering the transient nature of their interaction, it may be difficult to obtain cocrystal structures. To gain insight into the molecular details of their interaction, we here pursued an unbiased approach using phage display, peptide arrays, and different *in vitro* and *in vivo* interaction assays. These experimental approaches revealed the VirB8-interacting domain of VirB5 and of the very hydrophobic transmembrane protein VirB6. This general strategy will provide insights into the molecular details of protein–protein interactions in the absence of high-resolution structural information.

MATERIALS AND METHODS

Cultivation of Bacteria. The strains and plasmids used in this study are listed in Table 1 of the Supporting Information). Cultures of *Escherichia coli* JM109 for cloning experiments were grown at 37 °C in LB (1% tryptone, 0.5% yeast extract, and 0.5% NaCl) in the presence of antibiotics for plasmid propagation [100 µg/mL carbenicillin (car) and 50 µg/mL kanamycin (kan)]. For protein overproduction, *E. coli* strain GJ1158 was grown under aerobic conditions at 37 °C in LBON medium (1% tryptone and 0.5% yeast extract) to an OD₆₀₀ of 0.4–0.8, followed by the addition of 0.3 M NaCl. Cultivation under aerobic conditions proceeded at 26 °C for 16 h after induction. For phage propagation, *E. coli* ER2738 was used and grown at 37 °C using 20 µg/mL tetracycline.

Plasmid, Strain Constructions, and Mutagenesis. DNA manipulations followed standard procedures.³⁶ Site-directed mutagenesis and deletions of *virB5* were performed using pT7-7StrepIIVirB5 as a template for inverse polymerase chain reaction (PCR).³⁷ Here, the use of overlapping sequences of PCR primers (Table 2 of the Supporting Information) along with *DpnI* treatment of the PCR product at 37 °C for 2 h allowed direct cloning in *E. coli* without the need for ligation.

Purification of Fusion Proteins. N-Terminally StrepII-tagged proteins (VirB5 and derivatives and VirB8–VirB10) and H₆TrxAVirB8 were purified as described previously.⁴

Peptide Array Analysis. The methodology used for peptide array analysis was followed as described previously.⁵ The sequence of VirB5 from *Brucella suis* (GenBank accession number AAD56615) without the signal peptide was displayed on a cellulose membrane as N-terminally acetylated 13-mer

peptides covalently bound at the C-terminus. The sequence shifted by three amino acid positions each, beginning with peptide 1 (AHAQLPVTDAAGSI) and peptide 2 (QLPVTDAAGSIAQN), etc., to peptide 70 (YPQPKALEAAY). The protocol for “mapping of discontinuous epitopes” from the supplier was applied (Jerini, Berlin, Germany). The peptide array membranes were preincubated for 30 min in TBS-T [20 mM Tris-HCl, 137 mM NaCl, and 0.1% Tween 20 (pH 8.0)], transferred into blocking solution (Roche) for 1 h, washed with TBS-T for 10 min, and then incubated in a blocking solution containing the different proteins (VirB8–VirB10) at 1–5 µg/mL for 12 h at 4 °C. The membranes were then washed three times in TBS-T for 10 s to remove nonspecifically bound protein and transferred onto PVDF membranes with a semi-dry blot device (Fast-Blot, Biometra) followed by Western blotting.

Phage Display. Purified VirB8 was prepared in 0.1 M NaHCO₃ (pH 8.6) at a concentration of 100 µg/mL, adsorbed onto polystyrene microtiter plates (Thermo Scientific), and incubated at 4 °C for 16 h. This was followed by blocking for 2 h at 37 °C with blocking buffer [0.1 M NaHCO₃ (pH 8.6), 5 mg/mL BSA, and 0.02% NaN₃]. Phage libraries (Ph.D.-12 or Ph.D.-C7C) were diluted to 4 × 10¹⁰ pfu/mL from the original library (New England Biolabs) and added to the plate to allow binding, followed by washing using TBS-T and elution of VirB8 binding phage using 100 µL of elution buffer [0.2 M glycine-HCl (pH 2.1) and 1 mg/mL BSA]. Amplification of phage, phage separation, and titering were performed as described previously.³⁸ Single-stranded DNAs were isolated from 1.5 mL of individually isolated plaque supernatant using the QIAprep M13 kit (Qiagen). Forward 1 (5'-gtgacgatccgcgaagcgccct-3') and 96gIII primers (5'-ccctcatagttattagcgaacg-3') were used to perform PCR to amplify the DNA sequence encoding the peptide that is surface-exposed. Each PCR product was sequenced, and the encoded peptide sequence was identified. Unique peptides that bound to VirB8 were pooled and aligned with VirB5 and VirB6 protein sequences using the Relic server's MATCH program.³⁹ This program uses a default scoring window of 5 and threshold score of 13. Pairwise similarity is calculated for each scoring window of residues. A cutoff value of 13 within a scoring window of 5 residues is considered to be significant when it aligns with the target protein at a specific position.³⁹ We also used MatchScan (P. D. Pawelek, unpublished data) that allows calculation of peptide similarity using a wide range of residue windows and scores.

Sodium Dodecyl Sulfate–Polyacrylamide Gel Electrophoresis (SDS–PAGE) and Western Blotting. Cells and protein samples were incubated in Laemmli sample buffer (SB) for 5 min at 100 °C, followed by SDS–PAGE.^{40,41} Western blotting was performed following standard protocols,⁴² with VirB protein-specific antisera.

Assays for Protein–Protein Interactions: Pull-Down and Cross-Linking Experiments. Biochemical analyses of interaction of VirB5 with VirB8 fusion proteins via pull-down assays were conducted as previously described.⁴ In this study, we analyzed the ability of StrepII-tagged VirB5 variants to bind to His-tagged VirB8 in pull-down assays.

The competitive inhibition of VirB5–VirB8 cross-links and VirB8 dimerization were followed as described previously.⁴ To assess the potency of VirB5 peptides to impact protein–protein interactions, we added increasing amounts of peptide (0.05, 0.5, 5, and 25 nmol) to mixtures of VirB5 and VirB8 or to VirB8 (50 pmol each) and incubated at 22 °C for 30 min. The cross-linking agent DSS [disuccinimidyl suberate, 10 mM stock in

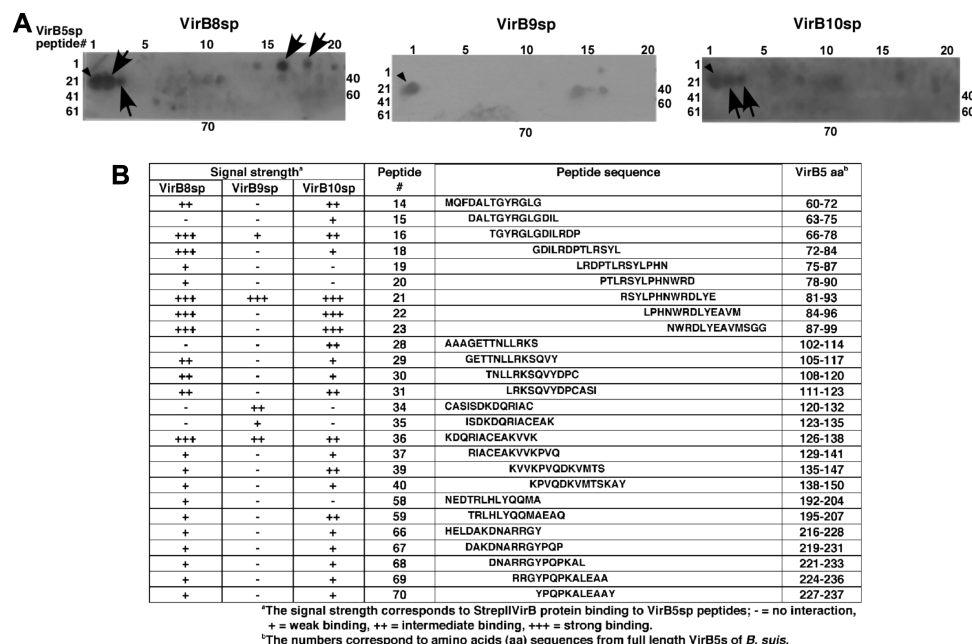


Figure 1. Identification of VirB8 binding peptides by a peptide array. (A) Binding of StrepII-tagged VirB8–VirB10 proteins to VirB5 peptides spotted on membranes was assessed by Western blot transfer of the bound proteins to PVDF membranes, followed by detection with specific antisera. Arrowheads indicate peptide 21 bound by all proteins, and arrows indicate reproducible strong binding to peptides by VirB8 and VirB10. The experiments were performed four to six times, and overlaid chemoluminograms are shown. (B) A code is used to indicate the intensity of VirB protein binding (PEP-Spot intensity) for every stretch of the corresponding VirB5 sequence. Signals from the Western blots were categorized to a certain peptide sequence as follows: –, no binding; +, weak binding; ++, intermediate binding; +++, strong binding. By alignment of the overlapping peptide, the sequence responsible for the observed signal (e.g., binding of VirB8) was identified.^{4,5}

DMSO (Pierce, Rockford, IL)] was added at a concentration of 0.1 mM; the mixtures were then further incubated for 1 h, and the reactions were stopped by the addition of 1 volume of SB, followed by SDS–PAGE and Western blotting. The four peptides used in the peptide competition assay (Jerini) corresponded to sequences from VirB5 [peptide I (TGYRGLGDILRDPTRL), peptide II (YLPNWRDLYEAVMS), peptide III (EAKVVKPVQDKVMTS), and peptide IV (ARRGYPOPKALEAAY)].

Bacterial Two-Hybrid Assay. Competitive inhibition experiments that aimed to examine the VirB8–VirB8 interaction in vivo using VirB5 peptides were conducted by using the bacterial two-hybrid system.⁴³ The full-length VirB8 protein was fused to the T18 and T25 fragments (catalytic domain of *Bordetella pertussis* adenylate cyclase) that were coexpressed in the BTH101 (*cya* deficient) cells.²⁹ The interaction was detected using the functional complementation between the two catalytic fragments that leads to the production of cAMP, which triggers β -galactosidase production detected using *o*-nitrophenyl β -D-galactopyranoside (ONPG) as the substrate. The VirB5 peptides were expressed N-terminally linked to the VirB5 signal peptide (SP) sequence for export into the periplasm and C-terminally tagged to tandem affinity tags, SC (strep tagII and calmodulin). To constrain folding, they were expressed as insertions in the thioredoxin A (TrxA) active site. This was performed by subcloning 5'-phosphorylated oligonucleotides into the unique *Rsa*II restriction site in the gene determining the active site of TrxA. To test the effects of the peptides on VirB8 dimerization, bicistronic constructs were created in the vector expressing VirB8 fused to the T18 fragment. The bicistronic constructs were then coexpressed with the T25–VirB8 fusion to analyze the effects of VirB5 peptides on VirB8 dimerization.

Protein Labeling. Conjugation reactions of Alexa Fluor 488 (A10254, Invitrogen) or Alexa Fluor 546 (A10258, Invitrogen) were performed according to the manufacturer's instructions. Briefly, 10 μ L of a freshly prepared aqueous solution of the dye (10 mg/mL) was added to previously reduced protein or peptide dissolved in 100 mM Tris-HCl (pH 7.3) and 150 mM NaCl. The reaction was allowed to proceed in the dark for 2 h at room temperature. Excess probe was quenched by adding a 100-fold molar excess of dithiothreitol and removed using a Sephadex G-25 prepacked Nap-5 column. The labeled product was further purified using a gel filtration Superdex 75 or Superdex Peptide column.

Fluorescence Measurements. Fluorescence emission spectra were recorded at room temperature in 100 mM Tris-HCl (pH 7.3) and 150 mM NaCl using a Cary Eclipse spectrofluorometer. The excitation wavelength was set to 488 nm, and spectra were recorded between 500 and 600 nm. Fluorescence resonance energy transfer (FRET) was assessed by the decrease in Alexa Fluor 488-labeled VirB8 fluorescence in the presence of Alexa Fluor 546-labeled peptide and calculated as $1 - F'/F$, where F' and F are the donor emission in the presence and absence of the acceptor, respectively. K_D values were calculated according to the method of Wang et al.⁴⁴ The VirB8 concentration was 20 μ M. The peptides used for the interaction assays contained an N-terminal Cys residue and corresponded to the VirB5 sequence (LGDILRDPTRLRSYLPHNWRDLYEA) and the VirB6 sequence [IGTSIHNQLNNVTMVASNTMNM (peptide I), DAFAGNHGTPSSTIYQTLDNSLGKGNIAAMLFEKGDNRGLT (peptide II), QIVQGFSELLSFLVAGSTLLAGPT (peptide III), and TSIFSGLSSGGSGSAKAGGESSYSAGGN (peptide IV)].

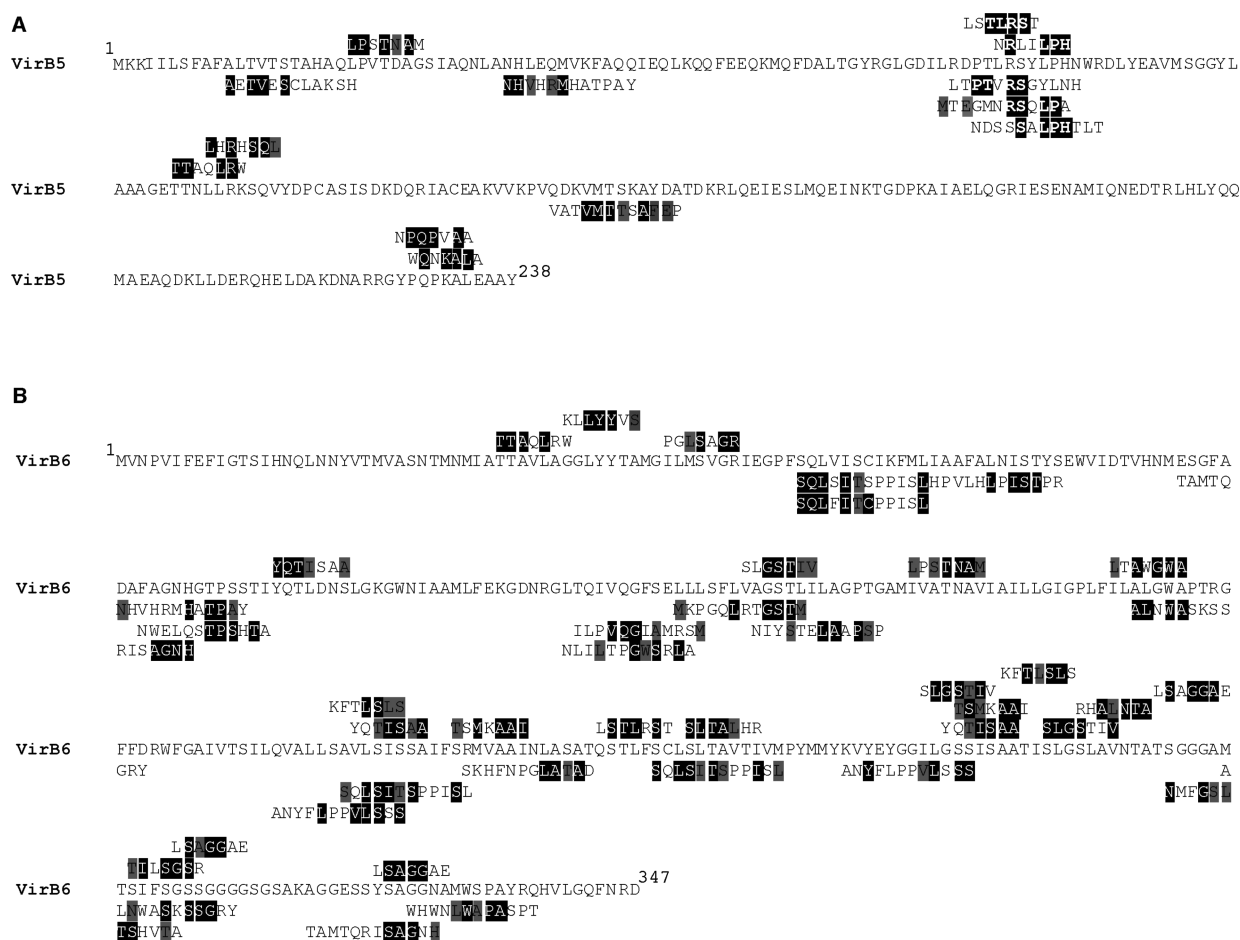


Figure 2. Identification of VirB8 binding peptides by phage display. Purified VirB8 protein was subjected to three rounds of panning using the Phage display library [Ph.D.-C7C and Ph.D.-12 (NEB)] and aligned with VirB5 and VirB6 protein sequences. The primary sequences of VirB5 (A) and VirB6 (B) are displayed with VirB8 affinity-selected peptides from Ph.D.-C7C and Ph.D.-12 libraries (NEB) aligned above and below, respectively. Identical residues in the protein and peptide sequences are highlighted in black, and conserved residues are highlighted in gray.

RESULTS

Peptide Array Analysis Identifies a Domain of VirB5 as a Site Interacting with VirB8. We have previously reported that VirB5 interacts with VirB8 and VirB10 but not with VirB9.⁴ An *in vitro* peptide array method was used to identify domains in VirB5 that are required for these protein–protein interactions. The sequence of VirB5 was displayed on cellulose membranes in “13-mers” shifting three amino acids each. After incubation of the peptide array membranes with interacting proteins (VirB8 and VirB10) and the negative control VirB9, the membranes were washed to remove nonspecifically bound protein and Western blot detection revealed the VirB5 peptides bound by VirB8–VirB10 (Figure 1A). The signal intensities of the proteins bound to the membranes were categorized from weak (+) and intermediate (++) to strong (+++) binding (Figure 1B). VirB8 and VirB10 bound a defined set of VirB5 peptides. In contrast, VirB9 reproducibly bound only to peptide 21, which was bound by all three proteins, and this is probably not specific. VirB8 and VirB10 interacted with peptides in VirB5 that were potential interaction partners, and we further pursued the analysis of the VirB5–VirB8 interaction in detail.

A Phage Display Approach to Identifying VirB8 Binding Peptides. To obtain independent evidence of VirB8 interaction partners and interacting domains, we next

used a phage display approach. Purified VirB8 was incubated with a library of M13 phages that displayed random 12-mer peptides on the surface of the pIII protein (Ph.D.-12) and 7-mer constrained peptides (Ph.D.-C7C), and binding phages were enriched by three rounds of panning. Single-stranded phage DNA was isolated, followed by PCR amplification, and sequenced to identify the surface-exposed peptide. We identified 140 unique peptides from both the Ph.D.-12 and Ph.D.-C7C libraries, and these were aligned with VirB protein sequences using the RELIC server MATCH program³⁹ and MatchScan (P. D. Pawelek, unpublished data). This analysis revealed potential interacting peptides on VirB5 and VirB6. Alignment of 140 unique peptides with VirB5 resulted in 13 peptides that had similarities (Figure 2A) and yielded a score that is either at the minimal threshold score of 14 or above (Table 4 of the Supporting Information). Interestingly, a cluster of peptides that were similar to VirB5 (amino acids 75–89) were localized in the globular domain of VirB5 that was modeled on the basis of the crystal structure of its homologue, TraC (Figure 7). This sequence overlaps with the peptides identified on peptide arrays and was therefore analyzed in more detail. In addition, phage display experiments identified potential interacting regions from the VirB6 protein that may also bind to VirB8 (Figure 2B). A total of 41 peptides displayed similarity to VirB6 (Figure 2B and Table 4 of the Supporting

Information). On the basis of the prediction of transmembrane topology, we studied the interaction of four peptides corresponding to the identified regions: a periplasmic N-terminal peptide (peptide I, amino acids 10–33), a periplasmic peptide located between transmembrane segments 2 and 3 (peptide II, amino acids 100–143), a peptide corresponding to the third transmembrane segment (peptide III, amino acids 144–169), and a C-terminal cytoplasmic peptide (peptide IV, amino acids 301–329) (Figure 7D). The unbiased screens using peptide array and phage display identified potential interaction partners and regions involved in their interactions with VirB8. We next tested these interactions using different *in vitro* and *in vivo* assays.

VirB5 Peptides from the Globular Domain Inhibit VirB5–VirB8 and VirB8–VirB8 Interactions. To assess the relevance of the VirB5 peptides identified by peptide array analysis as interaction site(s), we synthesized four of them and used them as competitors for the VirB5–VirB8 interaction. Peptide I (amino acids 66–80) and peptide II (amino acids 83–97) bound strongly to VirB8 in peptide array experiments (Figure 1). Peptide III (amino acids 133–147) and peptide IV (amino acids 224–238) bound barely detectable amounts of VirB8 in peptide arrays and were included as negative controls. To assess their ability to compete with the interaction, these peptides were added at increasing concentrations to samples for VirB5–VirB8 cross-linking experiments. This analysis showed that peptides I and II inhibited the formation of VirB5–VirB8 heterodimers as noted by the reduction of the 47 kDa cross-linking product (Figure 3A). In contrast, inclusion of peptides III and IV did not lead to a substantial reduction in the level of formation of the cross-linking product. This suggests that peptides I and II competed with the interaction between VirB5 and VirB8, and these results are consistent with those of the peptide array analysis. To assess the possibility of synergistic effects, peptides were combined and a mixture of peptides I and II had a stronger inhibitory effect than single peptides, suggesting that they are indeed part of the binding site for VirB8 (Figure 3B). In contrast, a mix of peptides III and IV did not inhibit cross-link formation, suggesting that they do not form part of the binding site.

It was interesting to note that the level of self-association of VirB8, as displayed by the formation of cross-linking products (dimerization and formation of higher-molecular mass complexes), also decreased in the presence of peptides I and II (Figure 3A). To assess whether this effect depends on the presence of VirB5, peptides I–IV were incubated with VirB8 in the presence of the cross-linking agent. Peptides I and II inhibited the formation of VirB8 cross-links, but peptides III and IV did not show such an effect (Figure 4A). These results suggest that VirB5-derived peptides impact the self-association of VirB8.

We next assessed whether the VirB5-derived peptides show a similar effect *in vivo* using a bacterial two-hybrid assay measuring the VirB8–VirB8 interaction via the restoration of fused domains of *Bordetella* adenylate cyclase, which leads to cAMP formation and induction of β -galactosidase as readout. In the presence of VirB5 peptides I and II expressed in the periplasm (pIpII-SC), we observed a significant reduction in the level of VirB8 self-association (Figure 4B). pIpII-SC contains both peptides I and II together, which likely present the residues necessary for interaction with VirB8 and therefore show a significant effect. In contrast, expression of peptide IV (pIV-SC) did not lead to a significant difference, which

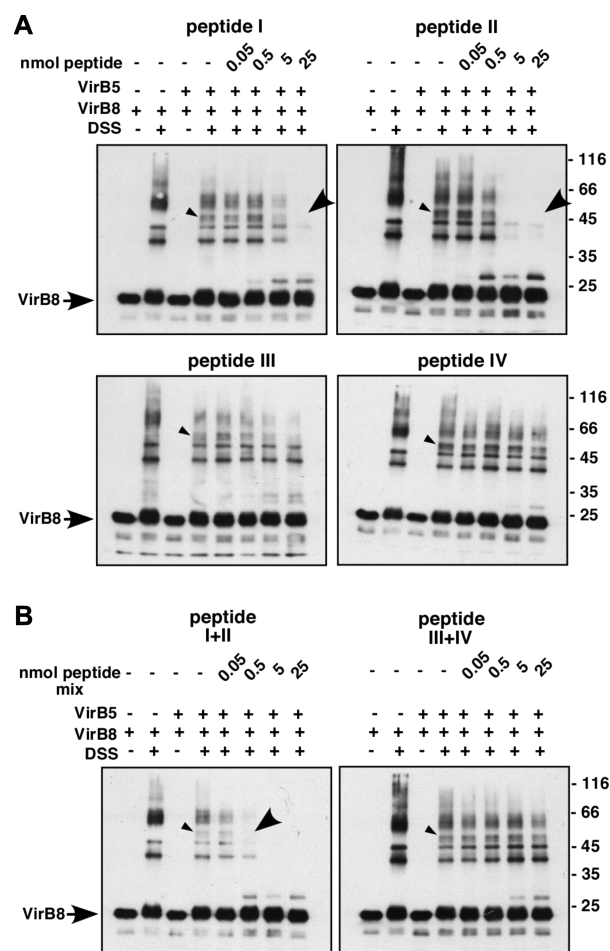


Figure 3. Peptide competition in the VirB5–VirB8 interaction. VirB5 and VirB8 were incubated with 0.1 mM DSS without and with an increasing amount of peptide (0.05, 0.5, 5, and 25 nmol) derived from the VirB5 sequence prior to SDS–PAGE and Western blotting with VirB8-specific antisera. (A) Effects of peptides I–IV were assessed individually. (B) The effect of combinations of peptides I and II vs peptides III and IV was assessed. The small arrowheads indicate the cross-link product of the VirB5–VirB8 interaction, and the large arrowheads indicate the reduced or abolished VirB5–VirB8 cross-link product.

corresponds with previous findings that peptide IV does not bind VirB8 and also does not compete with VirB8 self-association. To verify the importance of the globular domain of VirB5 for VirB8 binding in more detail, we next analyzed different variants of VirB5 with changes in or deletion of this domain.

Site-Directed and Deletion Mutagenesis of VirB5 Identifies Residues Critical for VirB8 Interaction *In Vitro*. As the next step of the structure–function analysis, we purified VirB5 deletion variants without the predicted globular domain (amino acids 71–138, StrepIIVirB5 Δ_{gb}) and the 18 amino acids from the C-terminus (StrepIIVirB5 Δ_{cd}) (abbreviated as Δ_{gb} and Δ_{cd} , respectively, in the following). We also purified five VirB5 variants with single-amino acid changes at positions conserved in VirB5-like proteins in the globular domain, which will be abbreviated by the change (e.g., L84A for VirB5 L84A). A pull-down assay was established, and to this end, we mixed His-tagged VirB8 with StrepII-tagged VirB5 variants, followed by a pull-down assay with Streptactin–Sepharose affinity beads to isolate the StrepII-tagged bait and bound VirB8

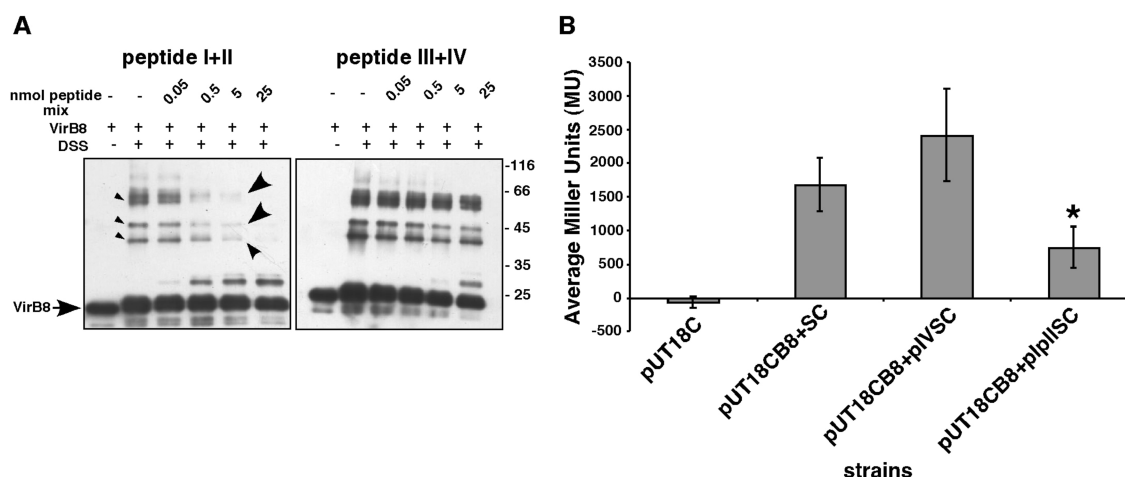


Figure 4. Inhibition of VirB8 self-association by VirB5 peptides. (A) In vitro assay. VirB8 was incubated in 0.1 mM DSS with an increasing amount of peptides (0.05, 0.5, 5, and 25 nmol) prior to SDS–PAGE and Western blotting with VirB8-specific antisera. The small arrowheads correspond to signals indicating VirB8 dimerization and formation of higher-molecular mass multimers, and the large arrowheads indicate the inhibition of VirB8 multimer formation by peptides I and II. The chemoluminograms corresponding to experiments with different peptides tested are indicated at the sides, and arrows indicate the monomeric VirB8. Molecular masses of reference proteins are shown at the right (kilodaltons). (B) Inhibition of VirB8 self-association by constrained VirB5 peptides in vivo. The bacterial two-hybrid assay showed that in the presence of peptides I and II (B8+pIpIISC) there is a significant reduction (asterisk) in the level of VirB8 self-association as determined by a *t* test in comparison to the wild type (B8+SC) or expression of peptide IV (pIVSC).

(Figure 5). This analysis showed that the globular deletion variant Δ gb did not interact with VirB8 while the Δ cd variant bound like the wild-type protein. In addition, we showed that four of the five variants bound VirB8 with reduced affinity (R69A, P85A, K138E, and D142A). These four amino acids are highly conserved and are localized either in or close to the predicted globular region of VirB5, which further supports the role of this domain in the interaction with VirB8.

A FRET Assay Shows Specific Interactions of Peptides with VirB8. As a final step of the analysis of VirB8 peptide interactions, we established a quantitative biochemical assay to measure binding. To this end, we selected a VirB5-derived peptide (amino acids 70–94) that includes the sequences of peptides I and II described above and four putative interacting VirB6-derived peptides (peptide I, amino acids 10–33; peptide II, amino acids 100–143; peptide III, amino acids 144–169; peptide IV, amino acids 301–329) that were identified by phage display (Figure 2). The peptides were synthesized with an N-terminal cysteine residue for modification with Alexa Fluor 546 C5-maleimide (FRET acceptor, Invitrogen), and the Q139C variant of VirB8 was modified with Alexa Fluor 488 C5-maleimide (FRET donor, Invitrogen).⁴⁵ Increasing amounts of labeled peptides were added to VirB8, and we observed a significant increase in the FRET efficiency with the VirB5 peptide (Figure 6A). The apparent K_D value was 75 μ M. In contrast, addition of three of the VirB6-derived peptides did not show energy transfer, but one of them, that corresponding to the large periplasmic loop between transmembrane segments 2 and 3 (Figure 7D), showed significant binding with an apparent K_D of \sim 100 μ M (Figure 6B). The specific binding of these peptides confirms that phage display and peptide arrays are suitable methods for the prediction of interacting domains and interacting partners of VirB8.

DISCUSSION

The work presented here provides insights into the structural requirements for the interaction between VirB8 and two essential T4SS components, VirB5 and VirB6. We have

previously demonstrated that purified *Brucella* VirB5 interacts with VirB8.⁴ In *A. tumefaciens*, VirB8 is necessary for formation of the T4SS complex and for its correct cellular localization.^{46–49} VirB8-like proteins may therefore act as assembly and nucleating factors and undergo transient interactions with several T4SS components.

In this study, we identified a novel interaction between VirB8 and a periplasmic loop of VirB6 (Figure 7D). VirB6-like proteins were characterized with different genetic and biochemical methods, but because of their high hydrophobicity, the purification has been very challenging and there is no structure available.^{30,31,50} Also, it is not clear what the actual role of VirB6 is, and there is no factual evidence that it functions as secretion pore. Deletion of *virB8* resulted in destabilization of many VirB proteins, including VirB6.^{4,51} Until now, all data suggesting an interaction with other T4SS components are rather indirect, but defects of VirB6 and VirB8 stop substrate translocation at the same step, suggesting that they work together.³³ The peptides we identified in this study by phage display provide evidence of VirB6 as an interacting partner of VirB8, and this was further confirmed by the finding that the periplasmic region of the VirB6 peptide interacts with purified VirB8 in FRET experiments (Figures 6A and 7D). The K_D of the interaction between the binding VirB6 peptide and VirB8 was calculated to be \sim 100 μ M, suggesting that the interaction is rather weak, although it may be enhanced by the presence of membrane domains of the full-length VirB6 protein and within a physiological context of bacterial membranes. Also, VirB8 is considered to be a T4SS assembly factor, and it is therefore consistent with its function that its interactions are transient and relatively weak. Nevertheless, the application of phage display followed by a biophysical approach (FRET assay) substantiates earlier studies that had indirectly suggested a VirB6–VirB8 interaction. This discovery places the VirB6–VirB8 complex at the center of T4SS assembly and substrate translocation.

In contrast to VirB6, much information is available on VirB5-like proteins that comprise a bundle of three α -helices and a globular appendage (Figure 7A). The secondary structure of VirB5 was deduced from the X-ray structure of TraC¹⁷ aided by

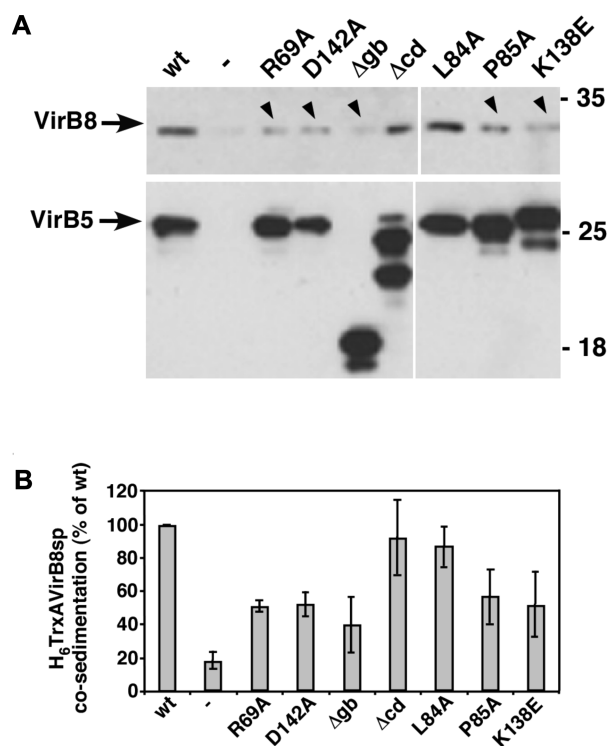


Figure 5. Affinity precipitation to test the interactions of VirB5 variants with VirB8. (A) StrepII-tagged VirB5 and variants were incubated with His-tagged VirB8 before addition of the Streptactin-Sepharose matrix. The proteins were sedimented with the matrix, followed by washing, elution of bound proteins, SDS–PAGE, and Western blotting with VirB5- and VirB8-specific antisera. The negative control of VirB8 incubated with the matrix is shown in the lanes labeled with a dash (–). Arrowheads indicate the VirB5 variants (amino acid changes and deletion of the globular domain Δgb), which cosedimented reduced amounts of VirB8 relative to wild type. Molecular masses of reference proteins are shown at the right (kilodaltons). (B) The ability of the VirB5 variants to bind to and cosediment VirB8 was quantified using densitometry of the chemoluminograms obtained with VirB8-specific antisera. The standard deviation was calculated using results from three independent experiments.

WebMol (<http://www.cmpharm.ucsf.edu/cgi-bin/webmol.pl>) and iMolTalk (<http://i.moltalk.org/>) to analyze the structural context of the results of this work (Figure 7B). The domain of VirB5 required for the interaction with VirB8 was identified

here. Peptide array and phage display showed that the globular region containing the 3₁₀ and α helix comprises VirB8 binding sites (Figure 7B,C). These results were substantiated by competition analysis with peptides from the globular region of VirB5. The formation of cross-links between VirB5 and VirB8 was inhibited by peptides (I and II) that correspond in sequence to the 3₁₀ and α helix. In contrast, negative controls with peptides III and IV derived from regions of VirB5 not bound strongly by VirB8 did not inhibit cross-link formation, suggesting that the results obtained with peptides I and II were not due to nonspecific competition. Mutational studies of TraC identified several residues important for incorporation into pili and for its function in plasmid transfer.¹⁷ We here analyzed the effects of similar changes introduced into *Brucella* VirB5, and four of them (R69A, P85A, K138E, and D142A) reduced the level of binding to VirB8 in pull-down assays, underlining the functional importance of this interaction. The VirB5 variants did not have major alterations in their overall structure as deduced by CD spectroscopy (not shown), suggesting the residues of this region contribute to VirB8 binding. Taking all the results together, we conclude that the minimal domain of VirB5 required for VirB8 binding is that of peptide I (TGYRGLGDILRDPTL) and peptide II (YLPHNWRDLYEAVMS) (Figure 7C). Changes at amino acid residues K138 and D142 also had a negative impact on binding to VirB8. The residue corresponding to D142 was identified as having a role for TraC functionality, which further supports the idea that this region is critical for protein function.¹⁷ However, peptide III, which encompasses the region of K138 and D142, was not bound strongly by StrepVirB8 and did not compete in vitro. We therefore conclude that this region between αd and the α2 helix is more likely to be required for correct orientation of the globular domain and not part of the VirB8 binding site.

We conclude that peptides I and II mimic the binding site of VirB8 on VirB5, and the results of the FRET-based interaction assay showing direct binding of this peptide to VirB8 confirmed this notion. In addition, the VirB5 peptide interacts with VirB8 with a K_D of ~75 μM, suggesting that this interaction may also be transient. Nevertheless, it is possible that other regions of VirB5 or amino acids flanking peptides I and II contribute to VirB8 binding. Similar to the rest of VirB5 (and VirB proteins in general), the region comprising peptides I and II is not highly conserved, but interestingly, it is believed to comprise an interaction site with

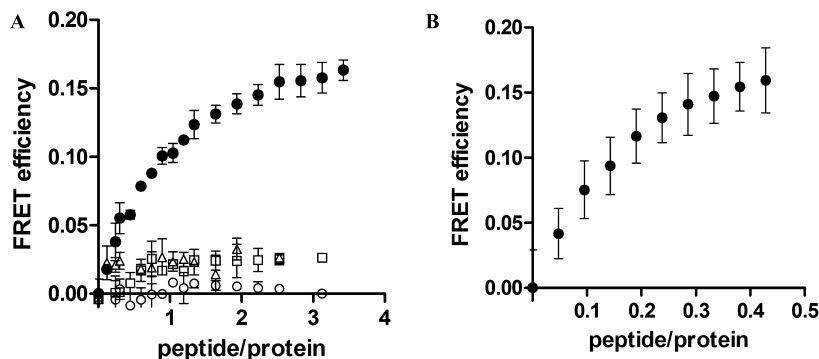


Figure 6. FRET assay to measure VirB8 peptide interactions. The fluorescence emission of Alexa Fluor 488 (donor) chemically attached to VirB8 was measured with increasing concentrations of peptides labeled with Alexa Fluor 546 (acceptor). The FRET efficiency was calculated as $1 - F'/F$, where F' and F are the donor emission in the presence and absence of the acceptor, respectively. (A) VirB6-derived peptides: (●) peptide II (amino acids 100–143), (△) peptide I (amino acids 10–33), (□) peptide III (amino acids 144–169), and (○) peptide IV (amino acids 301–329). The position of the different peptides within the VirB6 sequence is shown in Figure 7E. (B) Data for the VirB5-derived peptide (amino acids 70–94).

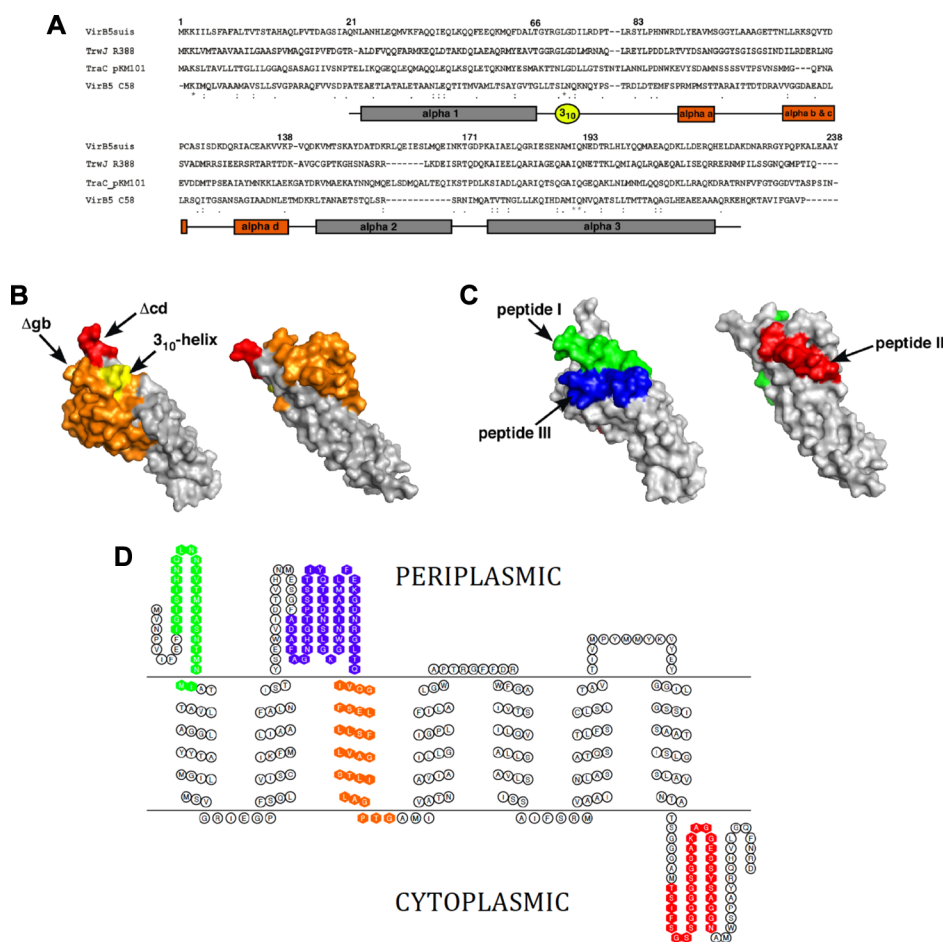


Figure 7. Localization of VirB8-interacting peptides on VirB5 and VirB6. (A) Alignment of amino acid sequences from four VirB5-like proteins (VirB5suis from *B. suis*, TrwJ from Inc.W plasmid R388, Trac from Inc.N plasmid pKM101, and VirB5agro from *A. tumefaciens*) using ClustalW (<http://clustalw.genome.jp/sit-bin/clustalw>). Asterisks denote amino acids identical in all sequences; colons denote conserved substitutions, and periods denote semiconserved substitutions. The secondary structure as predicted from the X-ray structure of Trac¹⁷ aided by WebMol (<http://www.cmpchem.ucsf.edu/cgi-bin/webmol.pl>) and iMolTalk (<http://i.moltalk.org/>) is displayed under the alignment, and colors are like those in panel B. (B) Surface representation of Trac in two different orientations showing the predicted localization of deletions introduced into VirB5 (Δ gb, globular domain deleted, colored orange; Δ cd, first residues of the deleted C-terminus colored red). The predicted location of the 3₁₀-helix is colored yellow. (C) Surface representation of Trac in two different orientations showing the predicted localization of the peptides used for competition experiments: peptide I (green, amino acids 66–80), peptide II (red, amino acids 83–97), and peptide III (blue, amino acids 133–147). Peptide IV (amino acids 224–238) is not visible as this portion of the C-terminus was not resolved in the X-ray structure of Trac. MacPymol (<http://pymol.sourceforge.net>) was used to generate the model of Trac based on Protein Data Bank entry 1R8I. (D) Peptides tested displayed on a model of the VirB6 structure generated with TOPO2 (<http://www.sacs.ucsf.edu/cgi-bin/open-topo2.py>) based on the transmembrane segment prediction using TMHMM (<http://www.cbs.dtu.dk/services/TMHMM/>): peptide I (green, amino acids 10–33), peptide II (blue, amino acids 100–143), peptide III (orange, amino acids 144–169), and peptide IV (red, amino acids 301–329).

surface receptors on host cells.^{17,52} The function of VirB8 is reminiscent of that of PapD, the periplasmic chaperone in the P-pilus system.⁵³ PapD forms soluble but transient complexes with pilin subunits, which stabilizes these proteins and targets them to the outer membrane-localized usher PapC. Whereas PapD has an immunoglobulin-like fold, VirB8 is structurally similar to protein binding factor NTF2,¹⁸ which mediates the translocation of protein to the nucleus. VirB8 could bind transiently to VirB5 and direct its interaction with VirB2 and incorporation into pili.^{4,51}

In the context of the cross-linking experiments, we made the interesting observation that peptides I and II also inhibited the formation of dimers and higher-molecular mass multimers of VirB8. Peptides III and IV did not have such an effect, suggesting that peptides I and II bind to VirB8 and prevent its self-interaction. Also, constrained peptides I and II showed significant reduction of the level of VirB8 self-association in an in vivo setting using the

bacterial two-hybrid assay. Formation of VirB8 dimers was proposed on the basis of protein contacts observed in the X-ray analysis^{18,35} and the results of cross-linking studies.⁴ We recently showed that VirB8 dimers form in vitro and that it is important for its functionality in vivo in the *Brucella* and *Agrobacterium* model systems.^{28,51} Peptides from the VirB8 binding site apparently mimic the action of VirB5 and dissociate the VirB8 dimer. This further substantiates our proposal that a dissociation–association cycle of VirB8-like proteins could be functionally important during its function as an assembly factor for VirB5 and other T4SS components.²⁹

■ ASSOCIATED CONTENT

Supporting Information

Tables with bacterial strains and plasmids, oligonucleotide sequences, phage display-identified peptides aligned with VirB5

using RELIC/MATCH and MatchScan, and phage display-identified peptides aligned with VirB6 using RELIC/MATCH and MatchScan. This material is available free of charge via the Internet at <http://pubs.acs.org>.

AUTHOR INFORMATION

Corresponding Author

*E-mail: christian.baron@umontreal.ca. Phone: (514) 343-6372.

Author Contributions

A.M.V.G. and D.S. contributed equally to this work.

Funding

This work was supported by grants to C.B. from the Canadian Institutes of Health Research (Grants MOP-64300 and MOP-84239), the FRQS-funded Groupe d'études des protéines membranaires (GÉPROM), the Canada Foundation for Innovation (CFI), the Fonds de recherche du Québec-Santé (FRQS), and European Union Frame Programme 5 (Contract QLK2-CT-2001-01200). A.P. was partly supported by a research fellowship from the German Deutsche Forschungsgemeinschaft (DFG).

Notes

The authors declare no competing financial interest.

ACKNOWLEDGMENTS

We thank Justin Deme from Dr. Coulton's laboratory for help with the alignment of VirB8 affinity-purified peptides and Dr. Peter Pawelek (Concordia University, Montreal, QC) for the use of MATCHSCAN.

REFERENCES

- (1) Llosa, M., and O'Callaghan, D. (2004) Euroconference on the Biology of Type IV Secretion Processes: Bacterial gates into the outer world. *Mol. Microbiol.* 53, 1–8.
- (2) Cascales, E., and Christie, P. J. (2003) The versatile bacterial type IV secretion systems. *Nat. Rev. Microbiol.* 1, 137–149.
- (3) Christie, P. J., Atmakuri, K., Krishnamoorthy, V., Jakubowski, S., and Cascales, E. (2005) Biogenesis, Architecture, and Function of Bacterial Type IV Secretion Systems. *Annu. Rev. Microbiol.* 59, 451–485.
- (4) Yuan, Q., Carle, A., Gao, C., Sivanesan, D., Aly, K., Höppner, C., Krall, L., Domke, N., and Baron, C. (2005) Identification of the VirB4-VirB8-VirB5-VirB2 pilus assembly sequence of type IV secretion systems. *J. Biol. Chem.* 280, 26349–26359.
- (5) Höppner, C., Carle, A., Sivanesan, D., Hoepfner, S., and Baron, C. (2005) The putative lytic transglycosylase VirB1 from *Brucella suis* interacts with the type IV secretion system core components VirB8, VirB9 and VirB11. *Microbiology* 151, 3469–3482.
- (6) Celli, J., and Gorvel, J. P. (2004) Organelle robbery: *Brucella* interactions with the endoplasmic reticulum. *Curr. Opin. Microbiol.* 7, 93–97.
- (7) Cascales, E., and Christie, P. J. (2004) *Agrobacterium* VirB10, an ATP energy sensor required for type IV secretion. *Proc. Natl. Acad. Sci. U.S.A.* 101, 17228–17233.
- (8) Dang, T. A., and Christie, P. J. (1997) The VirB4 ATPase of *Agrobacterium tumefaciens* is a cytoplasmic membrane protein exposed at the periplasmic surface. *J. Bacteriol.* 179, 453–462.
- (9) Dang, T. A., Zhou, X.-R., Graf, B., and Christie, P. J. (1999) Dimerization of the *Agrobacterium tumefaciens* VirB4 ATPase and the effect of ATP-binding cassette mutations on the assembly and function of the T-DNA transporter. *Mol. Microbiol.* 32, 1239–1253.
- (10) Lai, E.-M., and Kado, C. I. (1998) Processed VirB2 is the major subunit of the promiscuous pilus of *Agrobacterium tumefaciens*. *J. Bacteriol.* 180, 2711–2717.

- (11) Eisenbrandt, R., Kalkum, M., Lai, E. M., Lurz, R., Kado, C. I., and Lanka, E. (1999) Conjugative pili of IncP plasmids, and the T₄ plasmid T pilus are composed of cyclic subunits. *J. Biol. Chem.* 274, 22548–22555.
- (12) Jakubowski, S. J., Cascales, E., Krishnamoorthy, V., and Christie, P. J. (2005) *Agrobacterium tumefaciens* VirB9, an outer-membrane-associated component of a type IV secretion system, regulates substrate selection and T-pilus biogenesis. *J. Bacteriol.* 187, 3486–3495.
- (13) Schmidt-Eisenlohr, H., Domke, N., Angerer, C., Wanner, G., Zambryski, P. C., and Baron, C. (1999) Vir proteins stabilize VirB5 and mediate its association with the T pilus of *Agrobacterium tumefaciens*. *J. Bacteriol.* 181, 7485–7492.
- (14) Schmidt-Eisenlohr, H., Domke, N., and Baron, C. (1999) TraC of IncN plasmid pKM101 associates with membranes and extracellular high molecular weight structures in *Escherichia coli*. *J. Bacteriol.* 181, 5563–5571.
- (15) Krall, L., Wiedemann, U., Unsin, G., Weiss, S., Domke, N., and Baron, C. (2002) Detergent extraction identifies different VirB protein subassemblies of the type IV secretion machinery in the membranes of *Agrobacterium tumefaciens*. *Proc. Natl. Acad. Sci. U.S.A.* 99, 11405–11410.
- (16) Judd, P. K., Kumar, R. B., and Das, A. (2005) The type IV secretion apparatus protein VirB6 of *Agrobacterium tumefaciens* localizes to a cell pole. *Mol. Microbiol.* 55, 115–124.
- (17) Yeo, H.-J., Yuan, Q., Beck, M. R., Baron, C., and Waksman, G. (2003) Structural and functional characterization of the VirB5 protein from the type IV secretion system encoded by the conjugative plasmid pKM101. *Proc. Natl. Acad. Sci. U.S.A.* 100, 15947–15962.
- (18) Terradot, L., Bayliss, R., Oomen, C., Leonard, G., Baron, C., and Waksman, G. (2005) Crystal Structures of the periplasmic domains of two core subunits of the bacterial type IV secretion system, VirB8 from *Brucella suis* and ComB10 from *Helicobacter pylori*. *Proc. Natl. Acad. Sci. U.S.A.* 102, 4596–4601.
- (19) Hare, S., Bayliss, R., Baron, C., and Waksman, G. (2006) A large domain swap in the VirB11 ATPase of *Brucella suis* leaves the hexameric assembly intact. *J. Mol. Biol.* 360, 56–66.
- (20) Fronzes, R., Christie, P. J., and Waksman, G. (2009) The structural biology of type IV secretion systems. *Nat. Rev. Microbiol.* 7, 703–714.
- (21) Gomis-Ruth, F. X., Moncalian, G., Perez-Luque, R., Gonzalez, A., Cabezon, E., de la Cruz, F., and Coll, M. (2001) The bacterial conjugation protein TrwB resembles ring helicases and F1-ATPase. *Nature* 409, 637–641.
- (22) Yeo, H. J., Savvides, S. N., Herr, A. B., Lanka, E., and Waksman, G. (2000) Crystal structure of the hexameric traffic ATPase of the *Helicobacter pylori* type IV secretion system. *Mol. Cell* 6, 1461–1472.
- (23) Chandran, V., Fronzes, R., Duquerroy, S., Cronin, N., Navaza, J., and Waksman, G. (2009) Structure of the outer membrane complex of a type IV secretion system. *Nature* 462, 1011–1015.
- (24) Fronzes, R., Schafer, E., Wang, L., Saibil, H. R., Orlova, E. V., and Waksman, G. (2009) Structure of a type IV secretion system core complex. *Science* 323, 266–268.
- (25) Ward, D. V., Draper, O., Zupan, J. R., and Zambryski, P. C. (2002) Peptide linkage mapping of the *A. tumefaciens* vir-encoded type IV secretion system reveals novel protein subassemblies. *Proc. Natl. Acad. Sci. U.S.A.* 99, 11493–11500.
- (26) Das, A., and Xie, Y.-H. (2000) The *Agrobacterium* T-DNA transport pore proteins VirB8, VirB9 and VirB10 interact with one another. *J. Bacteriol.* 182, 758–763.
- (27) Baron, C. (2006) VirB8: A conserved type IV secretion system assembly factor and drug target. *Biochem. Cell Biol.* 84, 890–899.
- (28) Paschos, A., Patey, G., Sivanesan, D., Gao, C., Bayliss, R., Waksman, G., O'Callaghan, D., and Baron, C. (2006) Dimerization and interactions of *Brucella suis* VirB8 with VirB4 and VirB10 are required for its biological activity. *Proc. Natl. Acad. Sci. U.S.A.* 103, 7252–7257.
- (29) Sivanesan, D., Hancock, M. A., Villamil Giraldo, A. M., and Baron, C. (2010) Quantitative analysis of VirB8-VirB9-VirB10

interactions provides a dynamic model of type IV secretion system core complex assembly. *Biochemistry* 49, 4483–4493.

(30) Hapfelmeier, S., Domke, N., Zambryski, P. C., and Baron, C. (2000) VirB6 is required for stabilization of VirB5, VirB3 and formation of VirB7 homodimers in *Agrobacterium tumefaciens*. *J. Bacteriol.* 182, 4505–4511.

(31) Jakubowski, S. J., Krishnamoorthy, V., and Christie, P. J. (2003) *Agrobacterium tumefaciens* VirB6 protein participates in formation of VirB7 and VirB9 complexes required for type IV secretion. *J. Bacteriol.* 185, 2867–2878.

(32) Jakubowski, S. J., Krishnamoorthy, V., Cascales, E., and Christie, P. J. (2004) *Agrobacterium tumefaciens* VirB6 domains direct the ordered export of a DNA substrate through a type IV secretion system. *J. Mol. Biol.* 341, 961–977.

(33) Cascales, E., and Christie, P. J. (2004) Definition of a bacterial type IV secretion pathway for a DNA substrate. *Science* 304, 1170–1173.

(34) Aly, K. A., and Baron, C. (2007) The VirB5 protein localizes to the T-pilus tips in *Agrobacterium tumefaciens*. *Microbiology* 153, 3766–3775.

(35) Bailey, S., Ward, D., Middleton, R., Grossmann, J. G., and Zambryski, P. (2006) *Agrobacterium tumefaciens* VirB8 structure reveals potential protein-protein interactions sites. *Proc. Natl. Acad. Sci. U.S.A.* 103, 2582–2587.

(36) Maniatis, T. A., Fritsch, E. F., and Sambrook, J. (1982) *Molecular Cloning: A Laboratory Manual*, Cold Spring Harbor Laboratory Press, Plainview, NY.

(37) Ansaldi, M., Lepelletier, M., and Mejean, V. (1996) Site-specific mutagenesis by using an accurate recombinant polymerase chain reaction method. *Anal. Biochem.* 234, 110–111.

(38) Carter, D. M., Gagnon, J. N., Damlaj, M., Mandava, S., Makowski, L., Rodi, D. J., Pawelek, P. D., and Coulton, J. W. (2006) Phage display reveals multiple contact sites between FhuA, an outer membrane receptor of *Escherichia coli*, and TonB. *J. Mol. Biol.* 357, 236–251.

(39) Mandava, S., Makowski, L., Devarapalli, S., Uzubell, J., and Rodi, D. J. (2004) RELIC: A bioinformatics server for combinatorial peptide analysis and identification of protein-ligand interaction sites. *Proteomics* 4, 1439–1460.

(40) Laemmli, U. K. (1970) Cleavage of structural proteins during the assembly of the head of bacteriophage T4. *Nature* 227, 680–685.

(41) Schägger, H., and von Jagow, G. (1987) Tricine-sodium dodecyl sulfate-polyacrylamide gel electrophoresis for the separation of proteins in the range of 1 to 100 kDa. *Anal. Biochem.* 166, 368–379.

(42) Harlow, E., and Lane, D., Eds. (1988) *Antibodies: A laboratory manual*, Cold Spring Harbor Laboratory Press, Plainview, NY.

(43) Karimova, G., Pidoux, J., Ullmann, A., and Ladant, D. (1998) A bacterial two-hybrid system based on a reconstituted signal transduction pathway. *Proc. Natl. Acad. Sci. U.S.A.* 95, 5752–5756.

(44) Wang, Z. X., Kumar, N. R., and Srivastava, D. K. (1992) A novel spectroscopic titration method for determining the dissociation constant and stoichiometry of protein-ligand complex. *Anal. Biochem.* 206, 376–381.

(45) Smith, M. A., Coinçon, M., Jolicœur, B., Paschos, A., Lavallée, P., Sygusch, J., and Baron, C. (2012) Identification of the binding site of *Brucella* VirB8 interaction inhibitors. *Proc. Natl. Acad. Sci. U.S.A.*, submitted for publication.

(46) Kumar, R. B., Xie, Y.-H., and Das, A. (2000) Subcellular localization of the *Agrobacterium tumefaciens* T-DNA transport pore proteins: VirB8 is essential for assembly of the transport pore. *Mol. Microbiol.* 36, 608–617.

(47) Judd, P. K., Kumar, R. B., and Das, A. (2005) Spatial location and requirements for the assembly of the *Agrobacterium tumefaciens* type IV secretion apparatus. *Proc. Natl. Acad. Sci. U.S.A.* 102, 11498–11503.

(48) Aguilar, J., Cameron, T. A., Zupan, J., and Zambryski, P. (2011) Membrane and core periplasmic *Agrobacterium tumefaciens* virulence Type IV secretion system components localize to multiple sites around

the bacterial perimeter during lateral attachment to plant cells. *MBio* 2, e00218-00211.

(49) Aguilar, J., Zupan, J., Cameron, T. A., and Zambryski, P. C. (2010) *Agrobacterium* type IV secretion system and its substrates form helical arrays around the circumference of virulence-induced cells. *Proc. Natl. Acad. Sci. U.S.A.* 107, 3758–3763.

(50) Judd, P. K., Mahli, D., and Das, A. (2005) Molecular characterization of the *Agrobacterium tumefaciens* DNA transfer protein VirB6. *Microbiology* 151, 3483–3492.

(51) Sivanesan, D., and Baron, C. (2011) The dimer interface of *Agrobacterium tumefaciens* VirB8 is important for type IV secretion system function, stability and for association of VirB2 with the core complex. *J. Bacteriol.* 193, 2097–2106.

(52) Backert, S., Fronzes, R., and Waksman, G. (2008) VirB2 and VirB5 proteins: Specialized adhesins in bacterial type-IV secretion systems? *Trends Microbiol.* 16, 409–413.

(53) Sauer, F. G., Remaut, H., Hultgren, S. J., and Waksman, G. (2004) Fiber assembly by the chaperone-usheer pathway. *Biochim. Biophys. Acta* 1694, 259–267.